

## CAPABILITY OF NON LINEAR EDDY VISCOSITY MODEL IN PREDICTING COMPLEX FLOWS

Colombo E.\*, Inzoli F., Mereu R.

\*Author for correspondence

Energy Department,

Politecnico di Milano,

Piazza Leonardo Da Vinci, 32

20133 Milano,

Italy

E-mail: emanuela.colombo@polimi.it

### ABSTRACT

The research field of the study is related with turbulence modeling. The general objective is the implementation in a commercial code, of two equations Non Linear Eddy Viscosity Model (NLEVM) which removes Boussinesq linear approximation for the Reynolds stress tensor. The work described in the paper implements a second order k- $\epsilon$  model based over Shih, Zhu and Lumley (1993) [1] and Craft, Launder and Suga (1996) [2] in the finite volume commercial code ANSYS-FLUENT v. 6.3.26, by writing additional subroutines. The model has been validated through experimental and DNS data available in the literature. The benchmarks shown in this paper are the straight Square Duct [8] and the Backward-Facing Step [9, 10]. After the validation, the model has been used for predicting the flow behavior for complex industrial applications. The geometry used is similar to the bowl-shape downcomer of nuclear reactor. This is an application field of interest still under study by the same research group and an international consortium.

### INTRODUCTION

Turbulence modelling still today represents one of the key bottlenecks for increasing the potential of CFD to accurately reproduce complex flow fields. Many are the approaches followed to try overcoming the issue. Looking at the literature while DNS seems to raise a great interest in the academic field, LES starts being used with a certain frequency for research applied to industrial problem. In this study, due to the complexity of the geometry and physic with high Reynolds regime involved, a two equation models approach, with a non linear relationship between stress and strain has been considered.

In particular, the models based on the hypothesis of Boussinesq are not adequate for capturing the effects of the

inequality of the normal stresses of the Reynolds stress tensor, and therefore, can not predict, for instance, any secondary motions observed in the flow field of a square duct. Being able to predict such secondary motions in turbulent flows may increase the reliability of CFD results and their capability to reproduce the flow field behaviour associated with many engineering applications and increase the range of applicability for two equations turbulent models. These mentioned models are based on time averaged Navier-Stokes equations proposed, in 1895, by Reynolds. In the Reynolds averaging of the Navier-Stokes equations (RANS) a statistical average in time is done before solving them. To remove some of the limitation included in these models may contribute to improve their capability in predicting complex flow without increasing the computational costs, as it will happen with the other RANS closure models (e.g. Reynolds Stress Model) or with the LES approach.

### NOMENCLATURE

$Re_t = \frac{\rho k^2}{\mu \epsilon}$		Turbulent Reynolds number
$U_i$	[m/s]	Time averaged velocity component
$u_i$	[m/s]	Fluctuating velocity component
<i>Special character</i>		
$\delta_{ij}$		Kronecker delta
$k$	[m <sup>2</sup> /s <sup>2</sup> ]	Turbulent kinetic energy
$\epsilon$	[m <sup>2</sup> /s <sup>3</sup> ]	Turbulent kinetic energy dissipation rate
$\sigma_x$		Turbulent Prandtl number
$\sigma_\epsilon$		Closure coefficient of the transport equation of $\epsilon$

### THEORETICAL BASIS

#### Governing Equations

Engineering calculations and approximations, generally require a level of accuracy that need to be at least adequate for predicting the mean effect of the turbulent quantities.

Instantaneous fluctuations are not required to be solved since their influence on the mean quantities may be negligible in many situations. Therefore, for practical approach modelling the averaged turbulent transport quantities are accurate enough for knowing the mean distribution of the main flow characteristics and how turbulence influences them. In the RANS approach a statistical average in time is computed before solving them.

For an incompressible Newtonian fluid the governing equations for a turbulent flow (without body force) can be written in Cartesian tensor notation as:

$$\frac{D\rho}{Dt} = 0 \quad (1)$$

$$\frac{D\rho U_i}{Dt} = -\frac{\partial P}{\partial x_i} + \frac{\partial}{\partial x_j} \left[ \mu \frac{\partial U_i}{\partial x_j} - \overline{\rho u_i u_j} \right] \quad (2)$$

The averaging process produces a set of equations for the mean flow that is not closed and the problem of solving it is known as the turbulence closure problem.

Reynolds average approach to turbulence requires Reynolds stresses to be modelled in an appropriate way. Common methods based on eddy viscosity model, employ Boussinesq hypothesis that correlate linearly the deviatoric part of the Reynolds stress tensor to the strain rate of the mean flow. Moreover the trace of the tensor is, for incompressible flow, proportional only to scalar quantity, known as the mean turbulent kinetic energy:

$$-\overline{\rho u_i u_j} = \mu_t \left( \frac{\partial U_i}{\partial x_j} + \frac{\partial U_j}{\partial x_i} \right) - \frac{2}{3} \rho k \delta_{ij} \quad (3)$$

This simple hypothesis, used in many of the current implemented eddy viscosity models, moreover, implies the disadvantage of considering turbulence viscosity as a scalar quantity (implying an "isotropic" behaviour). Any models including this figure can not work properly where flow turbulence is dominated by high swirled flows or high bended geometry with secondary flows that can not be solved accurately with a linear relationship between strain and stress.

### Two equation models: the k-ε family

Two-equation models allow resolving the closure by solving differential transport equations: one for k, the turbulent kinetic energy, and a second one for another scalar. This second transported quantity may be selected to be the spatial length of turbulence  $L$  or any combination of the type  $k^m L^n$  is appropriate for such implementation. Turbulent kinetic energy transport equation is:

$$\frac{D\rho k}{Dt} = \frac{\partial}{\partial x_i} \left[ \left( \mu + \frac{\mu_t}{\sigma_k} \right) \frac{\partial k}{\partial x_i} \right] + P_k - \rho \varepsilon \quad (4)$$

where  $P_k$  is the turbulent kinetic energy production:

$$P_k = -\overline{\rho u_i u_j} \frac{\partial U_i}{\partial x_j} \quad (5)$$

In the model developed by Jones and Launder in 1972 [3], the k-ε model, the second equation is defined for the turbulent dissipation rate, defined as  $\varepsilon \propto \frac{k^{3/2}}{L}$ .

The transport equation can be written as:

$$\frac{D\rho \varepsilon}{Dt} = \frac{\partial}{\partial x_i} \left[ \left( \mu + \frac{\mu_t}{\sigma_\varepsilon} \right) \frac{\partial \varepsilon}{\partial x_i} \right] + c_{\varepsilon 1} \frac{\varepsilon}{k} P_k - c_{\varepsilon 2} \rho \frac{\varepsilon^2}{k} \quad (6)$$

In these equations, turbulent viscosity is defined by the Prandtl-Kolmogorov relation  $\mu_t = \rho C_\mu \frac{k^2}{\varepsilon}$ . The closure coefficients used for closing the model are taken from Launder and Sharma (1974) [4] and below reported:

$C_\mu$	$\sigma_k$	$\sigma_\varepsilon$	$c_{\varepsilon 1}$	$c_{\varepsilon 2}$
0.09	1.0	1.22	1.44	1.92

**Table 1** Closure coefficients for k-ε model

### Non-Linear Eddy-Viscosity Model

The Boussinesq hypothesis limitations have motivated the researchers' effort to find a more accurate form for defining the relation between the Reynolds-stress tensor and the mean flow quantities (mainly the strain rate tensor).

Such relation, adopted together with a two-equation model based on the k-ε formulation, constitutes a Non linear Eddy Viscosity Model (NLEVM). This approach is sometimes referred to as algebraic since it uses the Boussinesq hypothesis to compute directly the Reynolds stress tensor [5] as the product of an eddy viscosity and the mean strain-rate tensor without solving differential transport equation for the six independent components of the tensor.

In such a formulation, explicit definition of Reynolds stress components is given, preventing either the increase of computation costs associated with the additional transport equations that need to be solved either the usage of empiric algebraic correlation for each stress component.

The idea associated with EARSM models, was first introduced in 1975 by Pope [6], who mathematically derived a general non-linear constitutive relation starting from the generalized Cayley-Hamilton theorem and applying the invariant principles. A second order formulation for the stress-strain relationship is more adequate that a linear relationship to capture some important characteristic of complex flow [5].

The following equation shows a quadratic formulation for the stress-strain relationship common to all EARSMs:

$$-\overline{\rho u_i u_j} = -\frac{2}{3} \rho k \delta_{ij} + \mu_t S_{ij} - C_1 \mu_t \frac{k}{\varepsilon} \left[ S_{ik} S_{kj} - \frac{1}{3} \delta_{ij} S_{kl} S_{kl} \right] + C_2 \mu_t \frac{k}{\varepsilon} \left[ \Omega_{ik} S_{kj} + \Omega_{jk} S_{ki} \right] - C_3 \mu_t \frac{k}{\varepsilon} \left[ \Omega_{ik} \Omega_{kj} - \frac{1}{3} \delta_{ij} \Omega_{kl} \Omega_{kl} \right] \quad (7)$$

where the strain rate and the vorticity tensor are defined as follows:

$$S_{ij} = \left( \frac{\partial U_i}{\partial x_j} + \frac{\partial U_j}{\partial x_i} \right) \text{ and } \Omega_{ij} = \left( \frac{\partial U_i}{\partial x_j} - \frac{\partial U_j}{\partial x_i} \right) \quad (8)$$

In the last decade many correlations have been studied and various authors contributed to a second order expansion of the k- $\varepsilon$  model. In this work, the implementation by Shih-Zhu-Lumley model is used. This second order model is characterized by an explicit relationship linking  $C_\mu$  to the invariant S and  $\Omega$  of the strain rate and the vorticity:

$$C_\mu = \frac{2/3}{A_1 + S + \alpha\Omega} \quad (9)$$

$$\text{where } S = \frac{k}{\varepsilon} \sqrt{\frac{1}{2} S_{ij} S_{ij}}, \quad \Omega = \frac{k}{\varepsilon} \sqrt{\frac{1}{2} \Omega_{ij} \Omega_{ij}}$$

In particular, in the current study,  $A_1$  and  $\alpha$  value are set according to an experimental campaign [7] done at the THTLab of the University of Tokyo ( $A_1=3.9$ ,  $\alpha=0$ ).

It is interesting to note that all the three coefficients multiplying the second order factors in the quadratic formulation ( $C_1$ ,  $C_2$ ,  $C_3$ ), as reported in Tab. 2, present the same structure: they are proportional to the inverse of  $C_\mu$  and to the inverse of a cubic function of S. This structure, together with a non constant definition of  $C_\mu$ , derives from respecting realizability in the second order formulation of the stress-strain relationship.

$C_1$	$C_2$	$C_3$
$\frac{0.8/C_\mu}{1000+S^3}$	$\frac{11/C_\mu}{1000+S^3}$	$\frac{4.5/C_\mu}{1000+S^3}$

**Table 2** Closure coefficients for linear and non-linear terms

Realizability is provided when the non-negativity of the turbulent normal stresses is granted and Schwarz inequality is respected. Despite this is a physical and mathematical principle to be granted for avoiding unphysical results, many of the current implemented turbulence models do not contain it.

The damping function for the turbulent viscosity  $\mu_t$ , proposed by Wilcox [5] as function of the turbulent Reynolds number  $Re_t$ , is defined as:

$$f_\mu = \frac{0.024 + \frac{Re_t}{6}}{1 + \frac{Re_t}{6}} \quad (10)$$

## MODEL VALIDATION

The validation of a numerical model is a required step that allows the testing of the implementation over a number of experimental data available in the literature, in order to assure the reliability of the model.

The present model has been validated by using two test cases: the Square Duct and the Backward-Facing Step. The numerical results are compared at two different levels:

1. with experimental data available for evaluating accuracy.
2. with the numerical results obtained with some of the turbulence models already implemented in the commercial code used in order to understand the innovative contribution added by the present model. For this purpose the “realisable” formulation of the k- $\varepsilon$  due to T. H. Shih et al. (and referred to as “rke”) and the RNG formulation due to V. Yakhot and S.A. Orszag (referred to as “RNGke”) natively implemented in the code have been used as comparison.

The Square Duct presents the interesting feature of the secondary motions, that can be predicted only removing Boussinesq hypothesis.

The Backward Facing Step represents a severe test for a turbulence model. The phenomena induced by the presence of the step, generating a vortex and perturbing the boundary layers, involves high adverse pressure gradients and high deformation of the path line in more than one direction as well as high strain rate.

Many experimental and numerical data are present in literature showing that the turbulence models of the k- $\varepsilon$  family do not predict accurately the reattachment length.

## Experimental set-up

The validation with the Square Duct is referred to experimental data of Cheesewright et al. [8]. The Reynolds number based on the mean velocity flow  $U_b$  (centreline velocity) is  $Re_h = \frac{2 \cdot H \cdot U_b}{\nu} = 4410$ , where H is the half height

of the duct. The domain is characterized by periodic boundary conditions. For the Backward Facing Step experimental data are taken from Jovic and Driver [9] already used by Moin et al. in order to validate their DNS simulation [10]. Jovic and Driver have measured the profiles of velocity in a double expansion duct, with an expansion ratio equal to 1.2. The step is 0.96 cm high and is positioned at 40 h from the entrance of the duct and followed from a section of length 140 h. The Reynolds number, based on the height of the step and the free stream velocity  $U_0=7.72$  m/s which gives  $Re_h=5100$ . The profiles of velocity are carried out with a Laser Doppler Velocimeter (LDV).

## Numerical settings

In the straight Square Duct, a 3D model with a double axis of symmetry has been used, in order to simulate 1/4 of the full domain. The boundary conditions used are reported in Table 3.

In/Out	Periodic Condition
Wall	No Slip wall
Bounding Plane	Symmetry

**Table 3** Square duct boundary conditions

In the Backward Facing Step, the numerical simulation has been performed over a 2D model, applying a symmetry condition in the middle of the duct, with boundary conditions reported in Table 4.

In	Flat velocity profile of 7.72 m/s
Out	Pressure outlet
Wall	No Slip wall
Bounding line	Symmetry

**Table 4** Backward facing step boundary conditions

In both case the grid was generated by using squared cells and an adaption to the wall has been applied.

In order to acquire the independency of the results from the grid, the domain has been refined in the critical areas. Grid-results independency has been verified looking at the reattachment length  $x_r$  defined as the abscissa where the wall shear-stress goes to zero. The segregated approach has been used for solving Navier Stokes equations with a Second Order Upwind spatial discretization for both cases. The turbulence models implemented by the authors are: 1) a  $k-\epsilon$  models with new realizability and second order terms: (“2ordke”) and 2) a version of the previous with damping function on turbulent viscosity (“2ordke-lr”)

The wall region has been resolved using the Enhanced Wall Treatment approach, natively implemented in the code [11]. The convergence of the numerical solution was checked and considered appropriate when:

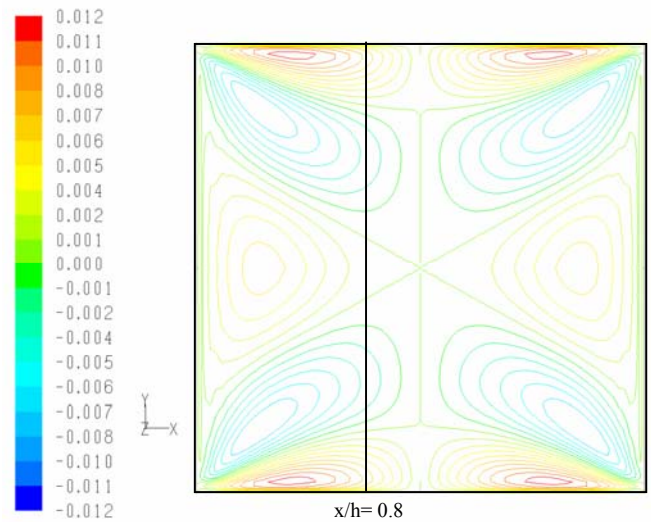
- the residuals are reduced at least of three orders of magnitude;
- the local values of selected quantities do not vary any more with the going on of the iterations;
- the total balance of mass is verified.

## VALIDATION RESULTS

### Square Duct

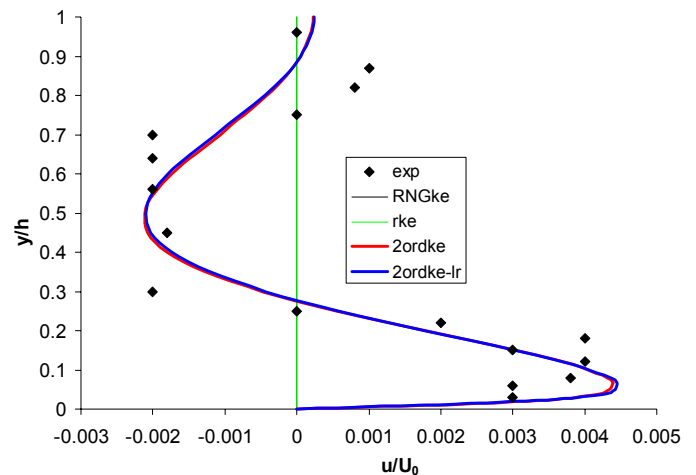
The flow in the Square Duct is characterised by the presence of the secondary motion developing in a plane orthogonal to the streamwise velocity. In a straight Square Duct the presence of the secondary motions of Prandtl are caused by turbulence and may be found in non circular section, and its magnitude is of the order of percentage of the main stream value. Such a motion, although of modest magnitude, can have important consequences in transporting towards the corner the fluid with high momentum, affecting the velocity profile of the flow.

Figure 1 shows that the flow, in a plane orthogonal to the direction of the motion, is characterized by the appearance of secondary flows with a magnitude roughly about 1% of the streamwise velocity ( $U_b$ ). Data from Gavrilakis DNS simulation shows a maximum magnitude of roughly 1.9% [12]. Despite a underestimation of the absolute value probably due to the low Reynolds number involved, the model is able to capture the location of the maximum.



**Figure 1** Contours of the adimensional velocity (x component) orthogonal to the flow field direction (z direction)

In figure 2 the adimensional span velocity profile in the cross section plane along a line close to the center ( $x/h=0.8$ ) is shown for comparing the implemented turbulence model with experimental data. It is evident, as it is well know, that the models based on the linear Boussinesq hypothesis (RNGke and rke) can not correctly predict such secondary flow (span velocity is zero along all the line), while a quadratic formulation proves to be adequate for capturing this feature.



**Figure 2** Adimensional velocity profile along a line ( $x/h=0.8$ )

### The Backward facing step

The step causes the separation of the boundary layer and its reattachment downstream. The separation point is fixed in correspondence of the abrupt expansion at the top of the step. In the flow field the following regions can be identified.

- a zone of development of the boundary layer along the duct up to the step;

- a shear layer, just downward the step, where viscous effects dominate;
- a zone of recirculation in which two counter rotating vortices are observed;
- a zone of reattachment of the flow induced by the adverse pressure gradient downstream the abrupt expansion;
- a recompression zone in which the boundary layer start again to develop over the wall.

Models	Reattachment	Error (%)
<i>Rke</i>	5.6 h	-8.2
<i>RNGke</i>	5.8 h	-4.9
<i>2ordke</i>	5.6 h	-8.2
<i>2ordkelr</i>	5.9 h	-3.3
<b>Exp. data</b>	6.1 h	

**Table 5** Reattachment lengths

The reattachment length, measured as the distance from the step where the wall shear stresses go to zero, has been used for validating the model (Table 6). All the models underestimate the experimental value, but the error is within the 10% .

In figure 3 the comparison between the numerical data and the experimental data for the Static Pressure Coefficient is given. Such coefficient is defined as  $C_p = \frac{2(p - p_0)}{\rho U_0^2}$  where  $p$

is the static pressure at the wall while  $p_0$  is a static reference pressure located at  $x/h = -5.1$  upstream the step.

The coefficient is plotted up to 10 h downstream the step where the recompression is nearly completed. It is interesting to note how the second order models show a better agreement with the experimental data in the zone of recirculation and in the area of recompression.

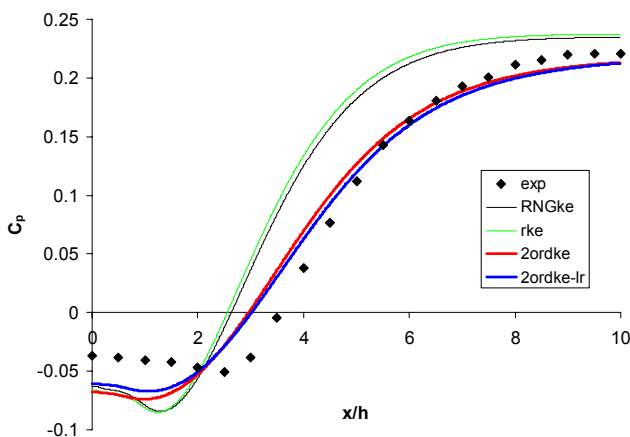


**Figure 3.** Static Pressure Coefficient along the bottom wall

## FURTHER APPLICATION

After the validation, the model has been applied to a more complex flow field and geometry in order to test its applicability to industrial problem.

No experimental data are here available and therefore this step may be done only after the validation phase. The results are given in terms of comparisons between the second order implemented model and the standard linear model of the same k-ε family.

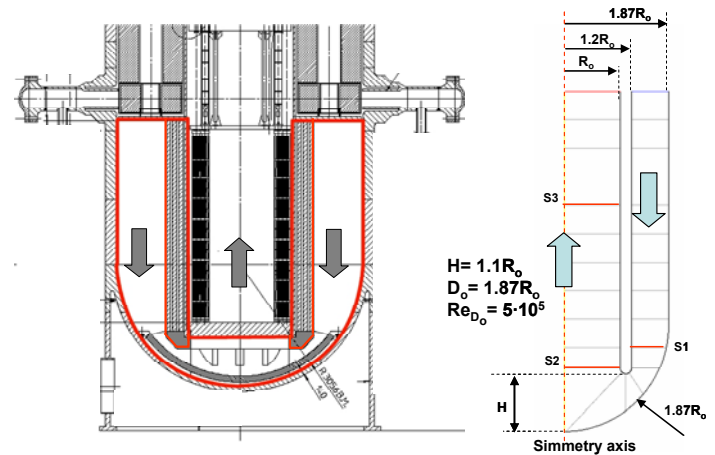


**Figure 4.** Domain geometry of IRIS downcomer and model

The geometry (figure 4) is similar to that of the downcomer lower plenum of the third generation (plus) nuclear reactor based on water technology (a tube bend with contraction and expansion area) and therefore presents characteristics which a linear relationship between strain and stress can not correctly simulate [13]. The Reynolds number based on internal flow model diameter  $D_o$  is equal to  $5 \cdot 10^5$ .

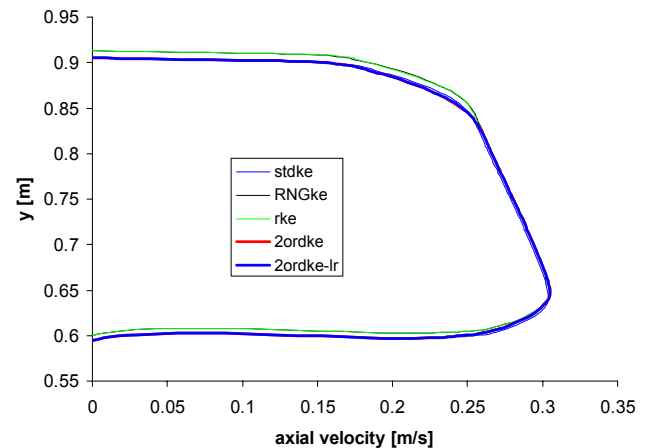


**Figure 5.** Axial Velocity along line “S1”. Line S1 is located  $1.5R_o$  from the downcomer lower apex

This assumption may be confirmed from the below figures where the difference in the obtained results between the model is relevant where results are sensitive to curvature effects. Indeed, Figure 5 shows the axial velocity before the bend and no significative differences may be underlined between linear

and second order models while figure 6, taken just after the bend as well as figure 7, taken in the region where the flow is still developing, show relevant differences.

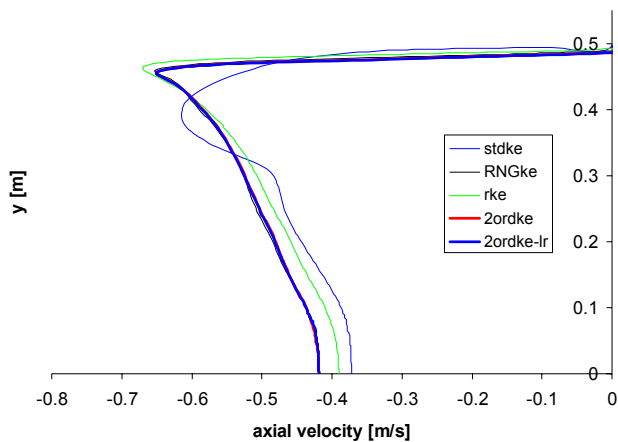


**Figure 6.** Axial Velocity along line "S2". Line S2 is located  $1.2R_0$  from the downcomer lower apex

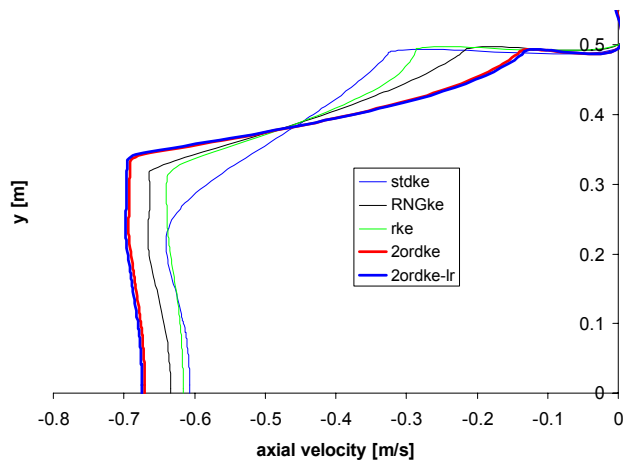


**Figure 7.** Axial Velocity along line "S3". Line S1 is located  $4R_0$  from the downcomer lower apex

Anyhow for a fully evaluation of the accuracy of the second order model, experimental data on the downcomer geometry would be required. Indeed, it is worthy to note that the consortium is nowadays working for preparing an experimental facility in order to set up a numerical and experimental system that can support the design and the licensing of the reactor.

## CONCLUSION

The model presented is a second order k- $\epsilon$  model based over Shih, Zhu and Lumley (1993) and Craft, Launder and Suga (1996) models. The model has been validated by using two different test cases: the Backward Facing Step characterised by the boundary layer separation and the Square Duct where secondary flows develop in a plane orthogonal to the streamwise direction. The implemented model with a

quadratic proposal for the stress-strain relationship is able to predict the secondary flow in a Square Duct and also to improve the prediction of the velocity profile in the zone of recirculation downstream the step. The introduction of the Wilcox damping function, add an additional benefit to the quadratic formulation of the stress-strain relationship, as shown in the results' section. By means of a comparisons with the RNG-k- $\epsilon$  and the Realizable-k- $\epsilon$ , natively implemented in the commercial CFD code used, it is possible to capture the distinguished figures associated with the non linear dependency of the stress-strain relationship compared to the linear hypothesis proposed by Boussinesq and this is also evident in the case study studied after validation which open further opportunity of application for the implemented model.

## REFERENCES

- [1] Shih, T.H., Zhu, J., and Lumley, J.L., A realizable Reynolds stress algebraic equation model, *NASA tech. memo, 105993*, 1993
- [2] Craft, T.J., Launder, B.E., and Suga, K., Development and application of a cubic eddy-viscosity model of turbulence, *Int. J. Heat Fluid Flow*, 17, 1996, pp. 108-115
- [3] Jones, W.P., Launder, B.E., The Prediction of Laminarization with Two-Equation Model of Turbulence, *Int. J. of Heat and Mass Transfer*, Vol. 15, 1972, pp. 301-314
- [4] Launder, B.E., Sharma, B.J., Application of the energy dissipation model of Turbulence of the calculation of flow Near a Spinning, 1974
- [5] Wilcox, D.C., Turbulence Modeling for CFD, DCW Industries, Inc. La Cañada, California, USA, 1998
- [6] Pope, S.B., A More General Effective-Viscosity Hypothesis, *J. of Fluid Mechanics*, vol. 72, 1993, pp. 331-340
- [7] Baglietto, E., Studies on Non-Linear Modeling in Computational Fluid Dynamics for Nuclear Engineering Applications, PhD Thesis, Tokyo Institute of Technology, Tokyo, Japan, 2004
- [8] Cheesewright, R., McGrath, G., Petty, D.G., LDA measurement of turbulent flow in a duct of square cross section at low Reynolds number. *Aeronautical Engineering Dept. Rep. ER 1011*. Queen May Westfield College, University of London, 1990
- [9] Jovic, S., Driver, D., Backward-facing step Measurements at low Reynolds Number, *NASA TM 108870*, 1994
- [10] Le, H., Moin, P., Direct numerical simulation of turbulent flow over a backward-facing step, *Journal of Fluid Mechanics*, Vol. 330, 1997, pp.349-374
- [11] FluentTM 6.3.26 User's Guide, Fluent Inc., 2007
- [12] Gavrillakis, S., Numerical simulation of low-Reynolds-number turbulent flow through a straight square duct, *J. Fluid Mech.*, vol. 244, 1992, pp. 101-129
- [13] Colombo, E., Inzoli, F., Ricotti, M., Uddin, R., Yan, Y., Sobh, N., Computational fluid dynamics as a support facility for R&D activities in the Iris project: an overview, 5th International Conference on Nuclear Option in Countries with Small and Medium Electricity Grids, Croatian Nuclear Society (HND) Ed., CD-Rom (ISBN 953-96132-8-0) , 2004, pp. 1-9